Available online at www.sciencedirect.com
SCIENCE DIRECT
Biochimica et Biophysica Acta 1758 (2006) 583–596
BIOCHIMICA ET BIOPHYSICA ACTA
BBA
http://www.elsevier.com/locate/bba

Photosensitization of skin fibroblasts and HeLa cells by three chlorin derivatives: Role of chemical structure and delivery vehicle

Fernando Postigo [a], M. Luisa Sagristá [a], M. Africa De Madariaga, Santi Nonell [b], Margarita Mora [a,*]

[a] *Departament de Bioquímica i Biologia Molecular, Facultat de Química, Universitat de Barcelona, Martí i Franquès 1, 08028-Barcelona, Spain*
[b] *Grup d'Enginyeria Molecular, Institut Químic de Sarriá, Universitat Ramon Llull, Via Augusta 390, 08017-Barcelona, Spain*

Received 18 July 2005; received in revised form 6 February 2006; accepted 13 February 2006
Available online 20 March 2006

Abstract

The chemical nature of the sensitizer and its selective uptake by malignant cells are decisive to choose an appropriate biocompatible carrier, able to preserve the photosensitizing characteristics of the dye. In this paper we demonstrate the photodynamic properties of three chlorins, derived from chlorophyll *a*, and the usefulness of liposomal carriers to design pharmaceutical formulations. The chlorins have been quantitatively incorporated into stable liposomes obtained from a mixture of L-α-palmitoyloleoylphosphatidylcholine and L-α-dioleoylphosphatidylserine in a 13.5:1.5 molar ratio (POPC/OOPS-liposomes). The chlorin uptake by skin fibroblasts increases steadily, reaching in all cases a plateau level dependent on both the chlorin structure and the vehicle employed. The photophysical properties of the three chlorins in THF are nearly identical and fulfill the requirements for a PDT photosensitizer. Incorporation of chlorins into liposomes induces important changes in their photophysics, but does not impair their cellular uptake or their cell photosensitization ability. In fact we observe in the cells the same photophysical behavior as in THF solution. Specifically, we demonstrate, by recording the near-IR phosphorescence of $^1O_2$, that the chlorins are able to photosensitize the production of $^1O_2$ in the cell membrane. The cell-photosensitization efficiency depended on the chlorin and cell line nature, the carrier, and the length of pre-incubation and post-irradiation periods. The high photodynamic activity of chlorin-loaded liposomes and the possibility to design liposomal carriers to achieve a specific target site favors this approach to obtain an eventual pharmaceutical formulation.

Keywords: Photosensitizers; Fluorescence lifetime; Photocytotoxicity; Singlet oxygen; Fibroblasts; HeLa cells

1. Introduction

The therapeutic properties of light have been employed in the treatment of disease for more than three thousand years. Nevertheless, the exploitation of their benefits in medicine comes about the last century with the development of photodynamic therapy (PDT) [1–3]. Photodynamic therapy involves the administration of a photosensitizing agent, followed by irradiation with visible non-thermal light (400–760 nm) to produce a series of cascade events eventually leading to the generation of reactive oxygen species. It may be employed in clinical oncology [4,5] for the treatment of other non-malignant conditions and many kind of skin afflictions [6–10], for virus inactivation [11], and for bactericidal purposes [12]. Besides these applications, drugs structurally related to photosensitizing agents are used in the detection of tumors by magnetic resonance imaging (MRI) [13,14].

Photodamage in PDT is described to occur by the so-called type I and type II mechanisms [15,16], depending on the kind of reaction undergone by the sensitizer after absorption of light. The electronically-excited state thus generated can react directly

Abbreviations: CHL-1, 3-Phorbinepropanol, 9,14-diethyl-4,8,13,18-tetramethyl-20-(3S-trans); CHL-2, 3-Phorbinepropanoic acid, 9,14-diethyl-4,8,13,18-tetramethyl-20-(3S-trans) (*meso*-pyropheophorbide *a*); CHL-3, 3-Methyl-phorbinepropanoate, 9,14-diethyl-4,8,13,18-tetramethyl-20-(3S-trans) (*meso*-pyropheophorbide *a* methyl ester); DMEM, Dulbecco's Modified Eagle's Medium; DMPC, L-α-dimiristoylphospatidylcholine; DPPC, L-α-dipalmitoyl-phosphatidylcholine; DMSO, dimethylsulfoxide; MB, methylene blue; MTT, 3-[4,5-dimethylthiazol-2-yl] 2,5-diphenyltetrazolium bromide; OOPS, L-α-dioleoylphosphatidylserine; PBS, Phosphate Buffered Saline; POPC, L-α-palmitoleoylphospathidylcholine; THF, tetrahydrofuran; TPP, 5,10,15,20-tetraphenyl-21*H*,23*H*-porphine; TPPS, 5,10,15,20-tetrakis(4-sulfonato)phenyl-21*H*,23*H*-porphine

* Corresponding author. Tel.: +34 93 4021212, fax: +34 93 4021559.
E-mail address: margarita.mora@ub.edu (M. Mora).

0005-2736/$ - see front matter © 2006 Elsevier B.V. All rights reserved.
doi:10.1016/j.bbamem.2006.02.027

with a biological target to produce radical species (type I reaction). Alternatively, it can transfer its energy to an oxygen molecule to form singlet oxygen ($^1O_2$), an electronically-excited, non-radical form of molecular oxygen (type II reaction). $^1O_2$ is highly reactive towards proteins, lipids, and nucleic acids, thus initiating oxidation chains that ultimately lead to the destruction of cells [4,5,15]. Formation of $^1O_2$ under photodynamic conditions has been demonstrated in vitro and in vivo [17].

The most efficiently-excited sensitizers are those which have strong absorption bands at the red end of the visible spectrum [18]. After the first-generation photosensitizer porfimer sodium received the approval by regulatory authorities, it became evident that there was a need for new compounds with improved photochemical properties and less side effects. Thus, a second-generation of photosensitizers with higher absorption coefficients in the 600–800 nm region and high quantum yields of singlet oxygen formation has been developed [11]. The compounds that have been more actively investigated include porphyrins, phthalocyanines, chlorins and bacteriochlorins, texaphyrins, and porphycenes [18]. Among them, chlorin derivatives, which differ from porphyrins only by saturation of a peripheral double bond of the macrocycle, are receiving considerable attention as potential drugs for photodynamic therapy. They have a considerable absorption in the so-called therapeutic window (650–900 nm), a fairly good triplet yield and show good tumor selectivity [19–21]. Nyman and Hynninen [22] have recently published an exhaustive review about the most recent advances in PDT, which considers the features and sources of different chlorins.

The efficacy of PDT is also determined by the selective localization of the photosensitizer in the malignant cells. Current trends focus on the development of the so-called third-generation photosensitizers [18], which are elaborated molecules, obtained from second generation compounds, with improved targeting mechanisms. This goal is achieved by incorporation into or attachment to chemical devices, e.g. by conjugation to monoclonal antibodies [23], by integration in the lipid bilayers of colloidal carriers such as liposomes [24], or by spatially isolation by an ionic dendrimer framework [25].

On the other hand, the most potent sensitizers are those that localize in photosensitive cellular compartments, particularly cell membranes where hydrophobic or amphiphilic sensitizers tend to accumulate. While hydrophobicity is an advantageous feature for PDT efficiency, it poses serious difficulties for drug administration through the blood stream, since hydrophobic sensitizers tend to aggregate in polar environments. Moreover, this aggregation results in a deterioration of the photophysical properties of photosensitizers, decreasing the photo-oxidation efficacy desired in photodynamic therapy [25]. This problem can be overcome by formulating the photosensitizers into suitable carriers, providing a biocompatible environment. For the purpose of in vitro studies but not for clinical applications, an expedient alternative is to solubilize the photosensitizer in organic solvent–water mixtures. DMSO is quite often the solvent of choice.

These considerations have pointed out the need for advanced delivery systems for PDT [26,27] and that both the sensitizer and the vehicle determine its efficacy [28,29]. There is an extensive literature about the use of drug delivery systems in the therapeutic treatments of many diseases [30]. It has been demonstrated that many of the pharmacological properties of conventional-free drugs can be improved through the use of drug delivery systems, which include polymer carriers, liposomes and bioconjugates [25,31,32]. Drug delivery systems are able to modify the pharmacokinetics and biodistribution of their associated drugs or to act as drug reservoirs. In this way, liposomes are especially useful carriers in the therapy of many diseases. In photodynamic therapy, it has been shown that liposomes increase the photosensitizing efficiency of some PDT agents by maintaining their monomeric form, by having a concentration effect, by modifying the uptake of the dye by malignant cells, or by influencing their subcellular location [33,34]. Indeed, Lavi et al. [35] have demonstrated the enhancement of the photosensitization process when the photosensitizer inserts their tetrapyrrole chromophore deeper into the liposomal lipid bilayer and the important effect of fluidization of the bilayer on the resulting photosensitization efficiency. Hydrophobic and amphiphilic photosensitizers entrapped into liposomes increase and sustain their clinical effects, reduce their toxicity, and are more protected from metabolism and immune responses [36]. Because of this, liposomes are considered valuable carriers to enhance the clinical effects of photodynamic treatments [37–39]. Different approaches to the design of liposomal carriers have been reported [40]. Passive versus active targeting or conventional versus surface-modified vesicles are criterions of choice to develop appropriate drug carriers for specific applications. Moreover, the carrier should ideally be able to incorporate the photosensitizer without loss or alteration of its activity. In this way, we have reported the lipid composition, method of liposome preparation, and structural features of photosensitizers for optimal incorporation into stable lipid vesicles. Special efforts have been devoted to prevent sensitizer aggregation in the lipid bilayer, since the ability of the liposome to solubilize the photosensitizer is dramatically decreased when it forms aggregates [41]. In addition, it has also been reported that only monomeric species and possibly planar end-to-end aggregates are endowed with significant photosensitizing ability [42].

Besides these remarks, it is of great interest in the field of anticancer therapy the consideration of the sensitivity of different cell lines to PDT. Thus, it seems that the effect of PDT depends on the sensitizer employed, but also on the cell type treated [43,44]. Zhang et al. [45] have shown that HeLa cells (a cervical adenocarcinoma cell line) are less sensitive to hypocrellin-A PDT than HIC (human intestinal cancer) and MGC-803 (mucoid gastric cancer) cells. Ahn et al. [46] also reported the effectiveness of PDT with the photosensitizing agent Photogem® against HeLa cells and pointed out that it might constitute an alternative to chemo- and radiotherapy, knowing the resistance of this type of tumor to these treatments. On the other hand, Tong et al. [47] have shown that at equivalent cellular Photofrin levels, Li–Fraumeni syndrome

cells (LFS cells) are more resistant than normal human fibroblasts to photofrin-mediated PDT, despite the fact that the uptake of photofrin per cell was greater in human fibroblasts cells than in LFS cells. In addition, different photodynamic effects of 5-aminolevulinic acid on neuroblastoma, hepatoma and fibroblast cells have also been reported [48]. The greatest sensitivity of neuroblastoma cells to ALA-PDT can be related to the high concentration of protoporphyrin IX and to the kinetics of protoporphyrin IX accumulation in this kind of cells.

Herein, we report on the photophysics, liposome encapsulation, cellular uptake, and photodynamic activity towards human fibroblast and HeLa cells of three chlorin photosensitizers derived from chlorophyll *a* (Fig. 1). The effect of two administration systems, DMSO and liposomes, are compared. Formation of singlet oxygen in the cells is unambiguously demonstrated.

2. Materials and methods

2.1. Chemicals

L-α-palmitoyloleoylphosphatidylcholine (POPC) and L-α-dioleoyl-phosphatidylserine (OOPS) were purchased from Avanti Polar Lipids (Birmingham, AL, USA). Polycarbonate membranes and imidazole were from Poretics Products (Livermore, CA, USA) and Sigma-Aldrich Chemical Co. (St. Louis, MO, USA), respectively. All other chemicals and solvents were of analytical grade. Solvents have been distilled before use. Milli-Q water (Millipore Bedford, Massachusetts system, resistivity of 18 MΩ cm) was used.

The porphyrins *meso*-5,10,15,20-tetraphenyl-21*H*,23*H*-porphine (TPP) and *meso*-5,10,15,20-tetrakis-(4-sulfonatophenyl)-21*H*,23*H*-porphine (TPPS) were purchased from Sigma-Aldrich Chemical Co. (St. Louis, MO, USA) and from Porphyrin Products (Logan, UT, USA), respectively, and were pure with a minimal grade of 99%. Tetrahydrofuran (THF) and methylene blue (MB) of the highest purity available were from Panreac Quimica S.A. (Barcelona, Spain).

Dulbecco's Modified Eagle's Medium with 4.5 g glucose/l (DMEM), fetal calf serum, penicillin-streptomycin solution and L-glutamine solution for biological assays were purchased from Biological Industries (Kibbutz Beit Haemek, Israel). Sterile Dulbecco's phosphate-buffered saline (PBS), dimethyl sulphoxide (DMSO) and 3-[4,5-dimethylthiazol-2-yl] 2,5-diphenyltetrazolium bromide (MTT) were purchased from Sigma-Aldrich Chemical Co. (St. Louis, MO, USA). The sterilized material was purchased from Techno Plastic Products (Trasadingen, Switzerland).

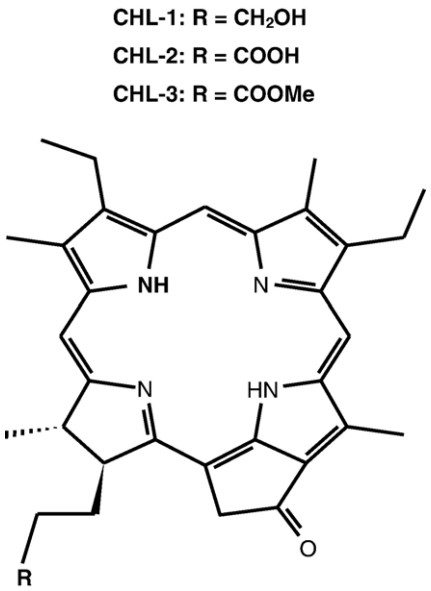

Fig. 1. Chemical structure of the three chlorin derivatives.

The three-chlorin derivatives were prepared for this project under guidance of Professor A. Vallès from the University of Barcelona. The synthesis followed published methods: CHL-3 is compound 3 in reference [49] and compound 7 in reference [50]. CHL-1 was obtained by removing the carbonyl protecting group of compound 11 in reference [49]. CHL-2 was obtained by acid hydrolysis of CHL-3. The structure of the compounds was verified by spectroscopy of ^{1}H-NMR, MS, and UV-Vis [51]. Purity of the chlorins was higher than 99.9% in all cases.

2.2. Preparation of liposomes

Encapsulation of all the chlorin derivatives in intermediate unilamellar liposomes (IUVs) was achieved by microemulsification following standard procedures as previously described [41]. Briefly, POPC/OOPS mixtures (13.5:1.5 molar ratio) at a lipid concentration of 10 or 20 mg/ml, alone or containing the photosensitizer at 15:1 or 30:1 lipid/chlorin molar ratio, respectively, were evaporated from a THF solution and kept in a vacuum desiccator for 12 h over P_2O_5 to remove the last traces of the solvent. 50 mM imidazole–HCl buffer (pH 7.4) was added to the dry film and the suspension (10–20 mg lipid/ml) was stirred by vortexing for 30 min (alternating 30 s of heating and 30 s of vortexing) at 45 °C to obtain MLVs. For singlet oxygen and some fluorescence experiments, the dry film was hydrated with pure D_2O instead. To prepare IUVs, the MLVs dispersions were frozen and thawed (five times), sonicated (bath sonicator, 60 min, 45 °C) and microemulsified (EmulsiFlex B3 device, Avestin, Ottawa, Canada). Microemulsification was carried out by pumping the fluid fifteen or thirty times through the interaction chamber (45 °C, 200 kPa) for 10 or 20 mg lipid/ml buffer, respectively. TLC analysis showed that the lipids did not suffer degradation during the sonication process. The absence of free photosensitizer in the liposomal systems, after centrifugation at 4000 rpm to eliminate the non-encapsulated dye, was checked by ultrafiltration (Centricon YM-30 Filter Devices, Millipore, USA) and by gel filtration (Sephadex G-50, Pharmacia Biotech, Uppsala, Sweden) of the liposomal suspensions as described previously [41].

2.3. Spectroscopic measurements

Absorption spectra were recorded on a Varian Cary 4E spectrophotometer. Absorption coefficients were determined from Beer–Lambert plots using at least three independent series of experiments. Fluorescence emission spectra were obtained using a Kontron SFM 25 fluorometer (Bio-Tek Instruments, Neufahrn, Germany). The fluorescence quantum yields were determined by comparison of the areas under the emission curves for optically-matched solutions of the chlorins and a reference, after correcting for the refractive index of the solvent (λ_{exc}=600 nm). Zinc(II) phthalocyanine was used as reference with Φ_F=0.30 [52]. The absorbance of the solutions was kept below 0.05 to prevent inner-filter effects. Fluorescence decays were recorded with a time-correlated single photon counting system (Fluotime 200, PicoQuant GmbH, Berlin, Germany) equipped with a red-sensitive photomultiplier. Excitation was achieved by means of a 654-nm picosecond diode laser working at 10 MHz repetition rate. The counting frequency was always below 1%. Fluorescence lifetimes were determined by analysis of the data using the PicoQuant FluoFit software. The Fluotime 200 was customized to detect the near-IR $^1O_2$ phosphorescence in the cells using a diode-pumped Nd:YAG laser (FTSS 355-Q, Crystal Laser, Berlin, Germany) working at 14 KHz pulse frequency and delivering 8 mW quasi-CW power at 532 nm for excitation. A near-IR sensitive photomultiplier tube with 300 ps TTS (H9170-45, Hamamatsu Photonics Deutschland GmbH, Herrsching, Germany) was used as detector. Photon counting was achieved with a Becker&Hickl (Berlin, Germany) MSA 300 board. The quantum yields of singlet oxygen production were determined using a 250-ns risetime Ge detector cooled at 77 K (EOL-817P, North Coast Corp., Santa Clara, CA) to detect the 1270 nm phosphorescence [53]. Samples were irradiated with a Continuum OPO laser (660 nm, 3 mm beam diameter, 5 ns pulsewidth, 0.1 to 1 mJ per pulse) pumped by the 3rd harmonic of a Continuum Surelite Nd:YAG laser. The detector output was captured with a Lecroy 9410 digital oscilloscope, and acquired by a PC computer for storage and analysis. Data recorded from 10 to 100 independent

laser pulses were averaged to improve the signal-to-noise ratio. The signal amplitude extrapolated to the end of the laser pulse was compared for the samples and for suitable references in air-saturated, optically-matched solutions in the same medium. Linearity of the signal amplitude with the energy of the laser pulsed was checked. TPP with $\Phi_\Delta = 0.66$ [54] was used in THF, and TPPS and MB, with $\Phi_\Delta = 0.67$ [55] and 0.52 [56], respectively, were used in D_2O-suspended liposomes. All spectroscopic measurements were carried out in 1-cm quartz cuvettes (Hellma, Germany) at room temperature and, in the case of cell suspensions, the samples were continuously stirred.

2.4. Liposome characterization

The photosensitizer content and the lipid concentration in the liposomes were evaluated following standard procedures as described previously [41]. Liposomes were disrupted by the addition of THF to an aliquot of the liposomal suspension, free of non-entrapped photosensitizer, obtained in imidazole–HCl buffer (THF/imidazole–HCl buffer, 24/1, v/v) and the absorbance was measured at the λ_{max} of the Soret band. The photosensitizer concentration was determined by comparison with standard curves obtained in the same conditions for each one of the different photosensitizers. The average size and polydispersity of unilamellar vesicles were determined by photon correlation spectroscopy (PCS) as previously described [41].

To control the stability of the preparations, the photosensitizer and lipid content in liposomes as well as the average size and polydispersity of the vesicles were also determined after storage up to 336 h.

2.5. Cell cultures

Human skin fibroblast cells (Foreskin cells, ATCC CRL-1635) and human HeLa cervical adenocarcinoma cells (ATCC CCL-2) were cultured at 37 °C in a humidified sterile atmosphere of 95% air and 5% CO_2 at 37 °C, using DMEM supplemented with fetal calf serum (10%, v/v), glucose (4.5 g/l), L-glutamine (292 mg/l), streptomycin sulfate (10 mg/l) and potassium penicillin (10 000 U/l). Human skin fibroblasts cells and HeLa cells were maintained frozen in DMEM with 10% DMSO. 1.8 ml CryoTubes™ (Nunc, Nalge Nunc International, IL, USA) were filled with the cellular suspension and then were placed in a cell Cryo 1 °C Freezing Container (Nalgene, Nalge Nunc International, IL, USA) to be slowly frozen up to −80 °C at a cooling rate of −1 °C/min for successful cell cryopreservation. Frozen cells were rapidly transferred to a liquid nitrogen container (−196 °C) and stored. Skin fibroblasts and HeLa cells are adherent cells which grow up to form cellular monolayers toward confluence after inoculation.

Human skin fibroblasts were seeded in 75 cm^2 tissue culture flasks (Techno Plastic Products, Trasadingen, Switzerland) and were cultured toward 80–85% confluence in order to control the uptake of chlorin derivatives by human skin fibroblasts. Nevertheless, to carry out cell photosensitization studies, both cell lines were inoculated in 96-well plates at a density of 10 000–15 000 cells/well and were cultured toward 90–95% confluence before beginning the experiment.

2.6. Cellular uptake

The cellular uptake of chlorin derivatives was estimated by flow cytometry, using Foreskin cells cultured in 75 cm^2 tissue culture flasks as indicated above. Chlorin derivatives, dissolved in DMSO or incorporated into liposomes, were added to the flasks at a concentration of 1 μM when a confluence of 80–85% was reached and the cells were incubated with each chlorin for different periods of time in the dark. Immediately after each time, the cells were washed with PBS to remove the non-entrapped chlorin. Trypsinization was carried out using PBS containing 0.2% trypsin and 0.5 mM EDTA. The suspension of cells was centrifuged at 1500 rpm for 5 min. The pellet was suspended in PBS and prior to flow cytometric analysis, the new suspension was filtered through nylon filters (Nytal, 70 μm mesh, Sefar Maissa S.A., Barcelona, Spain) to exclude cellular aggregates. Cells were analyzed for red fluorescence emission (670 nm) after excitation at 488 nm using a MoFlo High-Speed Cell Sorter (DakoCytomation, California, USA). The instrument was set up with the standard configuration. The excitation of the sample was performed with a standard 488-nm air-cooled argon-ion laser. The laser output power was set at 150 mW. Optical alignment was based on optimized signal from 10-nm fluorescent beads (Immunocheck, Epics Division, Coulter, FL, USA). Time was used as a control of the stability of the instrument. Red fluorescence was projected on a 1024 mono-parametrical histogram.

2.7. Cell photosensitization studies

Fibroblasts and HeLa cells were seeded in 96-well plates as indicated above and, when cell monolayers had reached a 90–95% confluence, the wells were inoculated with the appropriate amount of each chlorin derivative to obtain a photosensitizer concentration ranging from 1 to 10 μM in the wells. The cells were incubated for 1 or 24 h in the dark with the chlorins dissolved in DMSO or incorporated into liposomes. The cells were washed with PBS to remove non-entrapped chlorin and finally the buffer was replaced by the culture medium, supplemented as indicated above. Cell monolayers were then irradiated in DMEM for 36 min and 22 s, using a LED illuminator at 660 nm with a fluence of 7.2 J/cm^2.

The light dose and chlorin concentrations used in the phototoxicity studies were chosen on the basis of previous experiments, where the toxicity of the photodynamic treatment with different photosensitizers, among them CHL-1, towards red blood cells was assessed, bearing in mind that the administration route of our liposomal formulations would be the intravenous route [57]. Thus, the influence of the light dose and the photosensitizer concentration on red blood cells parameters after PDT was determined both in whole blood and red blood cells concentrates. In this way, experiments using CHL-1 concentrations ranging from 0.5 to 38 μM and light fluences of 1.4, 7.2, 14.4 and 21.6 J/cm^2 were carried out. The data obtained showed that a CHL-1 concentration up to 20 μM and a fluence up to 7.2 J/cm^2 will assure the integrity of red blood cells. According with this observation, we used the above mentioned chlorin concentrations of 1 μM to 10 μM and a fluence of 7.2 J/cm^2 to carry out the experiments reported in this paper.

After irradiation, the cells were incubated in the dark for different periods of time (0, 1, 2 and 24 h) before each assessment. The phototoxicity was next determined by the MTT colorimetric assay [58]. The cells were washed with PBS and 200 μl of DMEM, containing 2 mg MTT/ml, were added to each well. After 2-h incubation in the dark at 37 °C, the MTT solution was replaced by DMSO. The plate was finally vortexed for 10 min on a shaker and the absorbance at 550 nm was read on an ELISA microplate reader (ELISA System MIOS, Merck, Darmstadt, Germany). Photosensitization experiments were performed in triplicate and the samples without photosensitizers were used as negative controls. All experiments were performed in the dark to avoid unspecific photodynamic inactivation. The rate of phototoxicity was calculated as follows:

$$\%\ \text{MTT bioreduction} = \frac{\text{Abs}_{\text{sample}} - \text{Abs}_{\text{background}}}{\text{Abs}_{\text{control}} - \text{Abs}_{\text{background}}} \times 100 \quad (1)$$

where $\text{Abs}_{\text{sample}}$, $\text{Abs}_{\text{background}}$ and $\text{Abs}_{\text{control}}$ refer to the absorbance of the sample, the absorbance of the background (wells without cells) and the absorbance of the control (wells without photosensitizers), respectively.

3. Results

3.1. Photophysical properties of chlorins in solution

The photophysical properties of the photosensitizers were first determined in THF solutions in order to establish the basic properties of the compounds. Chlorins used in this work display a strong absorption band around 410 nm (the Soret band) and a series of weaker single Q bands in the 450–700 nm region of the visible spectrum (Fig. 2). Of specific interest for PDT, the lowest-energy band in the Q region, located around 660 nm, is also the strongest one with absorption coefficient ca. 4×10^4 M^{-1} cm^{-1}, 10-fold higher than those of porphyrins. These are typical features of chlorin photosensitizers [59]. The ratio

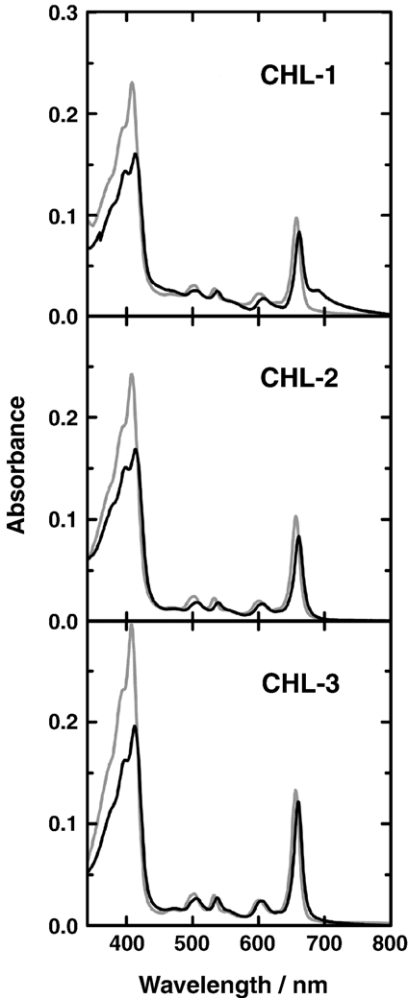

Fig. 2. Absorption spectra of 2.5 μM chlorin derivatives in THF (—) and in a suspension of POPC/OOPS liposomes (—). The molar ratio of lipid/chlorin was 15:1 for CHL-1 and CHL-2, and 30:1 for CHL-3.

absorbance/concentration was constant up to the highest concentration assayed, 100 μM, indicating that the chlorin derivatives are in monomeric form in this solvent. The addition of lipids caused a small but significant increase in the absorption coefficients (Table 1).

The fluorescence emission spectra show one intense band overlapping strongly with the lowest-energy absorption band and a smaller shoulder at ca. 710 nm (Fig. 3). The shape of the emission spectrum was independent of the excitation wavelength, consistent with the chlorin derivatives being present in monomeric form in THF solutions in agreement with the absorption-spectroscopy results. The area under the fluorescence spectrum for optically-matched solutions of the three chlorins was nearly identical, indicating that the fluorescence quantum yield is independent of the sensitizer structure. The fluorescence quantum yields compare favorably to values published for closely-related compounds [60]. The fluorescence decay of the three chlorins was strictly monoexponential in THF, with lifetime 6.9 ns, also independent of the sensitizer structure (Table 1 and Fig. 4).

The three compounds are able to sensitize the photoproduction of $^1O_2$ (Fig. 5). The quantum yield of $^1O_2$ photogeneration is close to 0.6, once again essentially independent of the sensitizer structure (Table 1). This value is typical for chlorin photosensitizers [61]. Overall, the photophysical properties of the three chlorins fulfill the requirements for a PDT photosensitizer.

3.2. Characterization of chlorin-loaded liposomes

The photosensitizer concentration in the liposomal systems was estimated spectrophotometrically, as indicated in Liposome characterization, using for each chlorin derivative the absorption coefficient (Soret band) obtained in THF solutions at the same lipid/photosensitizer molar ratio (Table 1).

Table 2 gives the incorporation efficiency for the different chlorin derivatives. The values at time 0 correspond to the lipid and chlorin content of freshly-prepared liposomal systems, whereas the values at 24, 168 and 336 h were determined to control the stability of the liposomal systems during storage. The data indicate that the incorporation efficiency of CHL-1 and CHL-2 into POPC/OOPS liposomes was near 100%, resulting in a final concentration of 8.7×10^{-4} M in the liposomal/buffer suspension. This concentration is ca. 10-fold higher than that used in typical liposome formulations [33,62]. While this affects the photophysical behavior of the chlorins in the liposomes (see below), we nevertheless favored this approach keeping in mind that an eventual pharmaceutical formulation should minimize the volume to be injected into a living organism. However, the percentage of incorporation obtained for CHL-3 was lower (70%, 6.1×10^{-4} M final concentration). On the other hand, the lipid content, expressed as the percentage of lipid in the sample relative to the lipid amount at the initial stage of the liposome preparation, was near 100% (ca. 10 mg lipid/ml liposomal dispersion), irrespective of the chlorin derivative used, thus preserving the 15:1 lipid/chlorin ratio for CHL-1 and CHL-2, and increasing it to 23:1 for CHL-3. These results indicate that there is a hindrance for the incorporation of CHL-3 into liposomal bilayers.

After 336 h storage, both the lipid and chlorin contents remained almost constant (>94%) in all cases, indicating that the liposomal dispersions are highly stable. Moreover, the liposomes containing CHL-3 are as stable as those containing CHL-1 and CHL-2 despite the lower incorporation efficiency of this chlorin.

Liposomes containing the three-chlorin derivatives at 15:1 lipid/photosensitizer molar ratio were also analyzed for average size and polydispersity by dynamic light scattering. The results, summarized in Table 2, show that the mean hydrodynamic diameter for the three liposomal systems was almost the same and remained constant during storage (135±12 nm). Thus, the nature of the photosensitizer does not modify the mean size of the vesicles. The results also confirm the stability of the liposomal systems. The polydispersity values, ranging from 0.25 to 0.40, are typical of the microemulsification method used to obtain the liposomes, which, in general, provides liposomal

Table 1
Photophysical properties of the chlorin photosensitizers in THF, POPC/OOPS liposomes, and human skin fibroblasts

Compound	CHL1			CHL2			CHL3		
Sample	THF	Liposomes	Fibroblasts	THF	Liposomes	Fibroblasts	THF	Liposomes	Fibroblasts
λ_{max}^{abs} (Q-reg) (nm)	657	661	–	656	661 [a]	–	656	662[a]	–
ε_{max} (Soret) (M^{-1} cm^{-1})	95400 97000 (L) [b]	–	–	96300 99000(L)[b]	–	–	110000 115000(L)[b] 120000(2L)[b]	–	–
ε_{max} (Q) (M^{-1} cm^{-1})	42400	–	–	43300	–	–	43700	–	–
λ_{max}^{flu} (nm)	657	661	–	656	660	–	656	658	–
Φ_F	0.45	0.13	–	0.42	0.13	–	0.47	0.24	–
Φ_F/Φ_F (THF)	1	0.28	–	1	0.32	–	1	0.52	–
τ_{flu} (ns)	6.9	3.5[c,d], 1.3[c,e]	7.3	6.9	3.6[c,d], 0.8[c,e]	7.3	6.9	6.7[c,d], 1.9[c,e]	7.4
Φ_Δ	0.63	0.18 [f]	–	0.65	0.19[f,g]	–	0.59	0.32[f]	–
Φ_Δ/Φ_Δ (THF)	1	0.29	–	1	0.29	–	1	0.54	–

λ_{max}^{abs}, wavelength of maximum absorption (±1 nm); ε_{max}, absorption coefficient at the maximum (±5%); λ_{max}^{flu}, wavelength of maximum fluorescence (±1 nm); Φ_F, fluorescence quantum yield (±10%); τ_{flu}, fluorescence lifetime (±5%); Φ_Δ, quantum yield of singlet oxygen production (±20%).

[a] Appears red shifted due to scattering.

[b] The absorption coefficient increases slightly upon addition of lipids at a chlorin/lipid ratio 1:15 (L) and 1:30 (2 L).

[c] Average lifetimes (see Table 3).

[d] In unbuffered H_2O.

[e] In 50 mM imidazole/HCl buffer (pH 7.4).

[f] In unbuffered D_2O.

[g] The same result was observed in POPC liposomes.

systems less homogeneous in size than other methodologies like extrusion.

In order to increase the amount of CHL-3 incorporated into the liposomal system, the amount of lipid was doubled. Thus, with a lipid concentration in the liposomal dispersion of 20 mg lipid/ml and an initial lipid/CHL-3 molar ratio of 30:1, the incorporation efficiency of CHL-3 increased to 97%. The lipid content, expressed as the percentage of lipid in the sample relative to the lipid amount at the initial stage of the liposome preparation, was near 100%, hence the lipid/CHL-3 molar ratio in the freshly-prepared liposomal systems was close to 30:1. The mean hydrodynamic diameter was 145±15 nm and remained almost constant after 336 h of storage (141±17 nm), showing again the stability of this new liposomal system.

In summary, the three chlorins have been quantitatively incorporated into liposomes, though CHL-3 required a double amount of lipid. The size of the liposomes is essentially independent of the chlorin nature and the suspensions are stable over long periods of time, allowing their storage.

3.3. Effect of liposome incorporation on the photophysical properties of chlorin derivatives

Incorporation of the chlorins into liposomes produced remarkable changes in their photophysical properties. The Soret and Q bands decreased their intensity and shifted slightly to the red. In the case of CHL-1, a shoulder appeared at the red end of the spectrum (Fig. 2).

Consistent with the changes in the absorption spectra, the fluorescence intensity decreased significantly for the three compounds. The fluorescence quantum yield of the chlorins in liposomes prepared in D_2O was, relative to its value in THF solution, 0.28, 0.32, and 0.54 for CHL-1, CHL-2, and CHL-3, respectively (Fig. 3). Likewise, the fluorescence decay kinetics showed a more complex pattern than in THF solutions. Thus, two to three exponential terms were needed to fit the fluorescence decay data (Fig. 4 and Table 3) and the average fluorescence lifetime was shorter than in THF. Moreover, it was shorter for CHL-1 and CHL-2 than for CHL-3 (Table 1). It is worth noting that the nature of the medium employed for the hydration of the lipid-chlorin film in the liposome preparation has additional effects on the fluorescence kinetics. Thus, when the aqueous phase contained imidazole/HCl 50 mM, the lifetimes decreased further relative to neat D_2O or phosphate buffer.

The lower fluorescence intensity and faster decay of the chlorins' singlet excited state in the vesicles suggests that they should produce singlet oxygen with lower efficiency than in THF solution. This is indeed the case (Fig. 5 and Table 1) and the ratios Φ_Δ (liposomes)/Φ_Δ (THF) are in excellent agreement with the ratios Φ_F (liposomes)/Φ_F (THF) values for the three chlorins (Table 1).

While the changes in the absorption spectrum could be attributed to the lipid environment [41], the decrease of the fluorescence and singlet oxygen quantum yields, and the complex fluorescence decay kinetics are likely the consequence of the high local concentration of the chlorins in the lipid bilayers (ca. 70 mM, roughly 4000-fold larger than in THF) [63], as suggested by similar observations for related macrocycles in lipid bilayers [42,64,65]. It is particularly revealing that CHL-3, with a lower 1:30 chlorin-to-lipid ratio, is clearly less affected (Fig. 2), even though it is possible that this differential behavior reflects a different site of localization within the lipid bilayer [35].

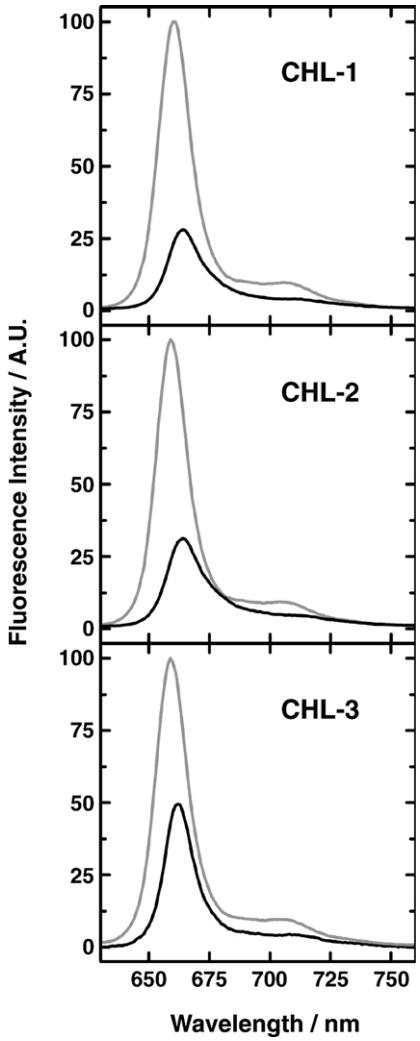

Fig. 3. Fluorescence spectra of 2.5 μM chlorin derivatives in THF (—) and in a suspension of POPC/OOPS liposomes (—). The molar ratio of lipid/chlorin in the liposomes was 15:1 for CHL-1 and CHL-2 and 30:1 for CHL-3. Samples were excited at 600 nm.

3.4. Chlorin uptake by skin fibroblasts

The incorporation of chlorin derivatives into human skin fibroblasts was measured by flow cytometry. Fig. 6 shows the fluorescence of the cells as a function of the incubation time. The chlorin uptake increases steadily, reaching a higher plateau level for CHL-1 than for CHL-2, and this one in turn slightly higher than for CHL-3. This differential behavior is observed irrespective of the vehicle used to deliver the chlorins, DMSO or liposomes. For any given chlorin, a higher uptake is observed when the photosensitizers are solubilized in DMSO (cf. Fig. 6A and B).

3.5. Chlorin photophysics in human skin fibroblasts

Because of its unparalleled sensitivity, fluorescence spectroscopy is the ideal tool to examine the behavior of the chlorins incorporated into fibroblasts. As shown in Fig. 4 and Table 1, the behavior of chlorins in the cells is closer to that in THF solution than to that in liposomes. Thus, the fluorescence decays are strictly monoexponential, with lifetimes slightly higher than in THF solution, indicating that the chlorins exist as isolated monomer species in the cells and that they experience a similar environment.

The delivery vehicle, DMSO or liposomes, has no influence whatsoever on the fluorescence results (data not shown). It may thus be expected that the properties observed in THF hold in the cellular environment. Specifically, we would expect the chlorins to act as good singlet oxygen sensitizers. Indeed, using an ultrasensitive singlet oxygen detection system we were able to record the phosphorescence of singlet oxygen at 1270 nm generated by cell-incorporated chlorins (Fig. 7). Thus, a signal is observed at 1270 nm growing with time constant 3.3 μs and decaying with lifetime 3.7 μs. The decay lifetime is close to the reported lifetime value for $^1O_2$ in H_2O, suggesting that $^1O_2$ is

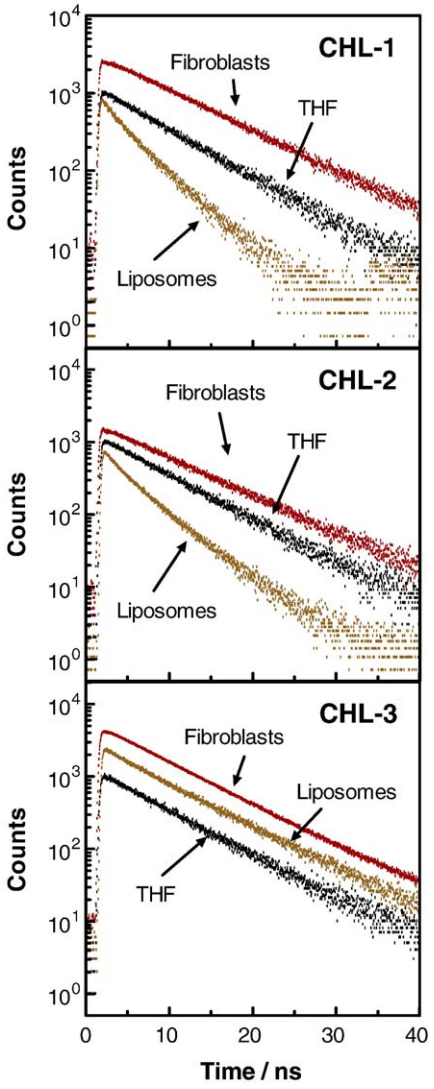

Fig. 4. Fluorescence decay of 16.45 μM chlorin derivatives in THF (—), in a suspension of POPC/OOPS liposomes (—), and in a suspension of human skin fibroblasts (—). The molar ratio of lipid/chlorin in the liposomes was 15:1 for CHL-1 and CHL-2 and 30:1 for CHL-3. Samples were excited at 654 nm and fluorescence was observed at 660 nm.

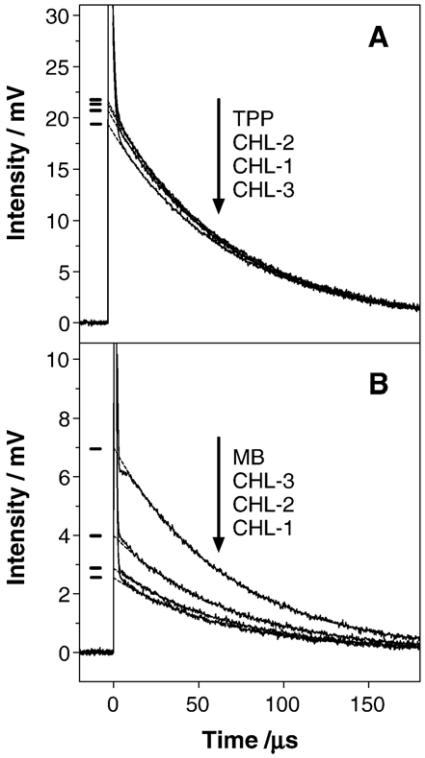

Fig. 5. Time-resolved 1270-nm $^1O_2$ phosphorescence photosensitized by optically-matched solutions of the chlorins and a reference sensitizer excited at 660 nm. A monoexponential function could appropriately fit the decay part of the transient (dashed line superimposed). The intensity at time = 0 (marked) is proportional to the $^1O_2$ quantum yield. (A) Decays in THF. The reference is TPP, with $\Phi_\Delta = 0.68$. (B) Decays in D_2O suspensions of POPC/OOPS liposomes. The molar ratio of lipid/chlorin in the liposomes was 15:1 for CHL-1 and CHL-2 and

able to diffuse out of the cell. The rise lifetime is comparable to those observed for triplet sensitizers in cellular environments [17].

In order to validate our interpretation of the signal the following control experiments were carried out. First, the luminescence was recorded at 1150 nm, where $^1O_2$ does not emit. At this wavelength, the signal disappeared, which confirms that the signal at 1270 nm was indeed caused by $^1O_2$. Second, we centrifuged the cells and analyzed the supernatant fluid at 1270 nm. No signal could be observed either, confirming that the signal at 1270 nm was caused by $^1O_2$ generated within the cell and not in the extracellular aqueous phase by a chlorin molecule that might had leaked from the cell [17].

Thus, the chlorins are able to photosensitize the production of $^1O_2$ in the fibroblasts and it can thus be expected that they will be able to photosensitize damage to these cells.

3.6. Photosensitization experiments of human skin fibroblasts

Studies on cell-photosensitization efficiency are summarized in Fig. 8. Human skin fibroblasts were treated with the chlorin derivatives either solubilized in DMSO or incorporated into POPC/OOPS liposomes. The cells were incubated with 1 μM chlorins for 1 or 24 h in the dark prior to photosensitization. Afterwards, the cells were exposed to red light using a LED illuminator at 660 nm with a fluence of 7.2 J/cm^2. The phototoxicity for human skin fibroblasts was assessed by the MTT assay at different post-irradiation times. It was observed that chlorin phototoxicity increased upon irradiation, as could be expected from the observed formation of singlet oxygen. Moreover, the chlorin nature, delivery vehicle, length of the pre-incubation period, and post-irradiation time affected cell photoinactivation in specific ways. Irrespective of the delivery vehicle used, all the chlorins were non-toxic in the dark (data not shown).

When cells were incubated with the chlorins for 1 h before irradiation (Fig. 8A and C), CHL-1 showed the highest photodynamic activity, irrespective of the delivery vehicle used and of the post-irradiation time. In all cases the order of effectiveness was CHL-1 ≫ CHL-2 > CHL-3, with cell photoinactivation as high as 95% for CHL-1 24 h after irradiation. For any given chlorin, the nature of the delivery vehicle had no influence on the 24 h phototoxicity; however, DMSO-delivered chlorins were more effective at early times.

In all cases, cell damage appeared earlier in cells incubated with the chlorins for 24 h (Fig. 8B and D) than in cells incubated with the sensitizers for only 1 h (Fig. 8A and C). In general, the extension and the rate of cell damage increased drastically when fibroblasts were incubated with the chlorins for 24 h before irradiation (Fig. 8B and D), consistent with the higher uptake of the drug (Fig. 6). The three chlorins were almost equally effective at inducing cell damage, irrespective of the delivery vehicle, as demonstrated by the similar phototoxicity observed 24 h after irradiation (see the 24-h bars in Fig. 8B and D; the only exception is CHL-2 in DMSO). In spite of the similar final phototoxicity, the time evolution of MTT bioreduction showed substantial differences among the photosensitizers and delivery vehicle used. Thus, in liposomes (Fig. 8B), CHL-1 caused almost complete damage immediately after irradiation, while for CHL-3, and especially for CHL-2, MTT bioreduction decreased more slowly. However, when DMSO was used, CHL-1 and CHL-3 showed a similar photodamage evolution, which was much faster than for CHL-2 (Fig. 8D). The incubation time before irradiation had a significant effect only on time evolution of the phototoxicity for CHL-3, when DMSO was used as delivery vehicle (see the CHL-3 bars in Fig. 8C and D).

3.7. Comparative photodynamic effects on human skin fibroblasts and HeLa cells

The photodynamic activity of CHL-1 was comparatively studied in two cell lines, human skin fibroblasts and HeLa cervical adenocarcinoma cells. The cells were incubated with different amounts of CHL-1 incorporated into POPC/OOPS liposomes for 1 h in the dark. Afterwards, the cells were exposed to red light using a LED illuminator at 660 nm with a fluence of 7.2 J/cm^2. Cell phototoxicity was assessed by the MTT assay 24 h after irradiation. The chlorin was ineffective in the dark irrespective of the cell line used (data not shown).

Table 2
Incorporation efficiency of chlorins in POPC/OOPS liposomes and stability of the liposomal systems

Sample	Time (h)	CHL [a] (%)	[CHL] (Molar)	Zave [b]
POPC/OOPS/CHL-1	0	96±2.0	$(8.6\pm0.2)\times10^{-4}$	123±28
(13.5:1.5:1)	24	93.0±3.2	$(8.4\pm0.3)\times10^{-4}$	123±15
	168	93.7±3.0	$(8.5\pm0.3)\times10^{-4}$	128±7
	336	93.2±2.3	$(8.4\pm0.2)\times10^{-4}$	128±6
POPC/OOPS/CHL-2	0	98.7±2.0	$(8.7\pm0.2)\times10^{-4}$	135±25
(13.5:1.5:1)	24	96.3±2.1	$(8.5\pm0.2)\times10^{-4}$	142±17
	168	94.3±3.7	$(8.3\pm0.2)\times10^{-4}$	139±6
	336	95.0±1.3	$(8.4\pm0.1)\times10^{-4}$	129±7
POPC/OOPS/CHL-3	0	70.4±4.8	$(6.1\pm0.4)\times10^{-4}$	145±17
(13.5:1.5:1)	24	72.1±3.0	$(6.2\pm0.5)\times10^{-4}$	132±17
	168	69.0±1.8	$(5.9\pm0.2)\times10^{-4}$	126±5
	336	65.8±2.6	$(5.7\pm0.2)\times10^{-4}$	128±9
POPC/OOPS/CHL-3	0	100±1.0	$(8.2\pm0.1)\times10^{-4}$	142±24
(27:3:1)	24	95.9±3.1	$(7.9\pm0.2)\times10^{-4}$	140±19
	168	97.2±2.8	$(8.1\pm0.2)\times10^{-4}$	135±10
	336	95.5±1.2	$(7.8\pm0.1)\times10^{-4}$	133±7

Liposomes were obtained in a 50 mM imidazole–HCl buffer (pH 7.4) at a lipid concentration of 10–20 mg/ml. The lipid/chlorin molar ratios, indicated in the table, were those used for liposome preparation.

[a] CHL: Chlorin derivative content, expressed as the percentage of the chlorin derivative in the sample with respect to the photosensitizer present at the initial stage of liposome preparation.

[b] *Z* average mean calculated from photon correlation spectroscopy data. Data are the mean values ± S.D. of three independent experiments.

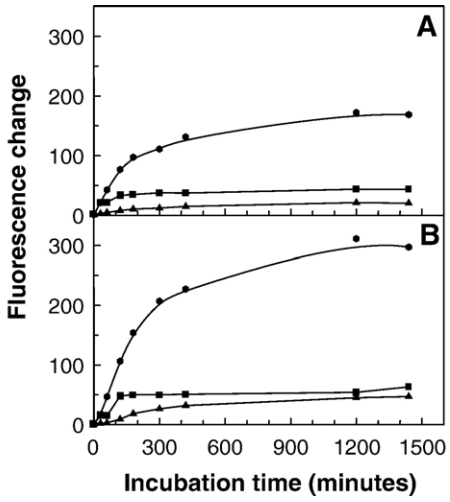

Fig. 6. Chlorin derivatives uptake by human skin fibroblasts. Human skin fibroblasts were incubated between 30 and 1440 min with CHL-1 (●), CHL-2 (■) and CHL-3 (▲) at 1 μM in the dark. Chlorin derivatives were added to the incubates incorporated into POPC/OOPS liposomes (A) or dissolved in DMSO (B). The molar ratio of lipid/chlorin was 15:1 for CHL-1 or CHL-2 and 30:1 for CHL-3. At different periods of time, cells were washed with PBS, trypsinized and centrifuged. The pellet was suspended in PBS and the cells were analyzed by flow cytometry. The transient increase in intracellular chlorin was recorded by monitoring the change in red fluorescence emission of the cells after excitation at 488 nm as a function of the incubation time with chlorins in the dark. Fluorescence change corresponds to the ratio between the fluorescence counts for each sample and for the control (without chlorins). Uptake experiments were performed in triplicate and CV values ranged from 4 and 16%.

Photodynamic treatment resulted in extensive cell death for both cell lines. Fig. 9 shows the cell phototoxicity as a function of the CHL-1 concentration. As can be observed, the LD_{50} in HeLa cells (2 μM) is ca. 5-fold higher than in human skin fibroblasts (0.4 μM). Moreover, the concentration of CHL-1 needed to decrease the MTT bioreduction of HeLa cells below 5% is 10 μM, 10-fold higher than that needed to produce the same damage to fibroblasts.

4. Discussion

The photodynamic effect has been extensively studied and its therapeutic benefits have been clinically proved [2–12]. From a pharmaceutical point of view, the chemical nature of the sensitizer [11] and its selective uptake by malignant cells [30,33,35,37–39] must be taken into account when choosing an appropriate biocompatible carrier. The present paper reports on the study of the potential of three chlorins, derived from chlorophyll a, for photodynamic therapy as well as on the usefulness of their incorporation into liposomes in order to obtain a colloidal biocompatible carrier for pharmaceutical formulations.

The three chlorins assayed (CHL-1, CHL-2 and CHL-3) have been quantitatively incorporated into POPC/OOPS liposomes, though CHL-3 required a double amount of lipid (20 mg lipid/ml) than CHL-1 and CHL-2 (10 mg lipid/ml). The size of the liposomes is essentially independent of the chlorin nature and the suspensions are stable over long periods of time, allowing their storage. The final concentration of the chlorins in the liposomal/buffer suspensions was, in all cases, near 8.0×10^{-4} M, which is ca. 10-fold higher than that used in typical liposome formulations [33,62]. This increase in the sensitizer concentration should minimize the volume to be injected into a living organism from an eventual pharmaceutical formulation.

The area under the fluorescence spectrum for optically-matched solutions in THF of the three chlorins was nearly identical and the fluorescence decay of the three chlorins was

Table 3
Fluorescence decay in liposome suspensions. The fluorescence intensity $I(t)$ was fitted to the equation $I(t)=\sum_i A_i\exp(-t/\tau_i)$

Sample	CHL1			CHL2			CHL3		
Fluorescence decay lifetimes	τ_1/ns (A_1/%)	τ_2/ns (A_2/%)	τ_3/ns (A_3/%)	τ_1/ns (A_1/%)	τ_2/ns (A_2/%)	τ_3/ns (A_3/%)	τ_1/ns (A_1/%)	τ_2/ns (A_2/%)	τ_3/ns (A_3/%)
POPC/OOPS liposomes in unbuffered H_2O	4.4 (67%)	1.6 (33%)	–	4.7 (65%)	1.7 (35%)	–	7.3 (89%)	2.1 (11%)	–
POPC/OOPS liposomes in imidazole/HCl buffer	2.3 (17%)	0.9 (41%)	0.2 (42%)	1.8 (5%)	0.6 (39%)	0.2 (56%)	3.7 (23%)	1.8 (49%)	0.5 (28%)

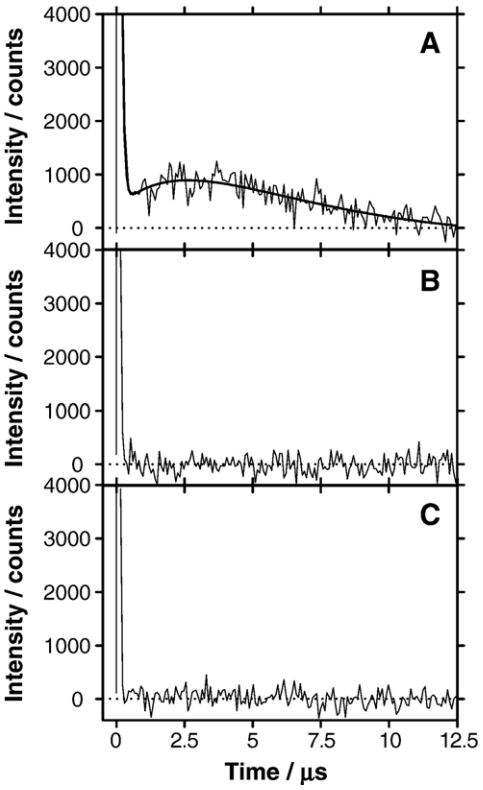

Fig. 7. Time-resolved $^1O_2$ phosphorescence from an H_2O-suspension of human skin fibroblasts loaded with CHL-1. The chlorin was excited at 532 nm. (A) Emission wavelength set at 1270 nm. A signal is clearly visible with rise-time 3.3 µs and decay-time 3.7 µs, consistent with $^1O_2$ located mainly in an aqueous environment. (B) Emission wavelength set at 1150 nm. The slow signal has disappeared, consistent with the lack of phosphorescence of $^1O_2$ at this wavelength. This confirms the assignment of the 1270-nm signal to $^1O_2$. (C) Emission wavelength set to 1270 nm. The cell suspension has been centrifuged and the supernatant, extracellular aqueous phase is now analyzed. The absence of signal demonstrates that $^1O_2$ was produced in the cell and was able to diffuse to the external aqueous phase within its lifetime.

strictly monoexponential in THF, with lifetime 6.9 ns (Table 1). Moreover, the three compounds are able to sensitize the photoproduction of $^1O_2$ (Fig. 5), with a quantum yield for $^1O_2$ photogeneration close to 0.6, (Table 1), which is typical for chlorin photosensitizers [60]. These results show that, in THF solution, the fluorescence quantum yield, the fluorescence decay and the $^1O_2$ photogeneration quantum yield are essentially independent of the sensitizer structure and indicate that the photophysical properties of the three chlorins fulfill the requirements for a PDT photosensitizer.

The incorporation of the chlorins into liposomes produced remarkable changes in their photophysical properties. Thus, the Soret and Q bands decreased their intensity and shifted slightly to the red, the fluorescence intensity decreased significantly for the three compounds and the fluorescence decay kinetics showed a more complex pattern than in THF solutions. Two to three exponential terms were needed to fit the fluorescence decay data obtained for chlorins incorporated into liposomes (Fig. 4 and Table 3) and the average fluorescence lifetimes in liposome-buffered suspensions were shorter than in THF (Table 1). Moreover, liposomal-trapped sensitizers produce singlet oxygen with lower efficiency than in THF solution. While the changes in the absorption spectrum of chlorins incorporated into liposomes could be attributed to the lipid environment [41], the decrease of the fluorescence and singlet oxygen quantum yields, and the complex fluorescence decay kinetics are likely the consequence of the high local concentration of the chlorins in the lipid bilayers as suggested by similar observations for related macrocycles in lipid bilayers [42,64,65]. An estimation for such concentration can be made by assuming that the volume occupied by one molecule of lipid is roughly 0.5 $nm^2 \times 3$ nm = 1.5 nm^3. Thus, the chlorin:lipid ratio 1:15 corresponds roughly to a concentration of 1 molecule of chlorin per 23 nm^3 of lipid environment or ca. 70 mM, 4000-fold larger than in THF.

The chlorin uptake by skin fibroblasts increases steadily, reaching a higher plateau level for CHL-1 than for CHL-2, and this one in turn slightly higher than for CHL-3. Moreover, irrespective of the chlorin nature, the uptake was higher when the sensitizer was added to the flask cultures dissolved in DMSO than incorporated into liposomes. These results agree with the faster intake of other photosensitizers by mouse tissues [66] or by Jurkat cells [67] when DMSO was used as delivery vehicle instead of liposomes. Wang et al. [66] showed that for a specific tissue the initial sensitizer intake was higher when its administration was carried out from a DMSO solution, as we observe in our cell cultures. Rancan et al. [67] indicate that, in general, sensitizers delivered in liposomes reach lower intracellular concentrations than those delivered in ethanol or DMSO solutions. On the other hand, the higher uptake of CHL-1 relative to CHL-3 is in line with the results obtained by Rancan et al. working with other chlorins [67], which showed that the most amphiphilic dye, with the highest affinity for hydrophilic/hydrophobic interfaces, exhibits the best uptake according to its higher ability to pass easily through the phospholipid bilayer. The lower uptake for the polar anionic chlorin CHL-2 can be attributed to the electrostatic barrier created by the negative membrane potential.

It could seem that DMSO solutions should be preferred over liposome suspensions as delivery vehicles in view of the negative effects of liposomes on the photophysical properties of the sensitizers and on their cellular uptake. However, solutions containing more than 30% DMSO are not pharmaceutically-acceptable formulations and such concentration is not enough yet to solubilize our hydrophobic chlorins. In contrast, liposomes are biocompatible and the high chlorin concentration (0.4 mg/ml) achieved by us makes them attractive for pharmaceutical purposes. For comparison, Photofrin is administered at 2.5 mg/ml. Indeed, verteporfin, a hydrophobic photosensitizer currently marketed under the trade name Visudyne, is formulated as a liposomal suspension [18,68]. Moreover, Wang et al. [66] reported a higher exclusion of the hypocrellin A sensitizer out of the tissue when DMSO was used relative to liposome formulations, concluding that liposomal formulations increase the sensitizer amount in tumor tissues and, as a consequence, achieve higher tumor regression. A third point to consider is that the chlorins exist as monomers in the cells, as demonstrated by the same photophysical properties as

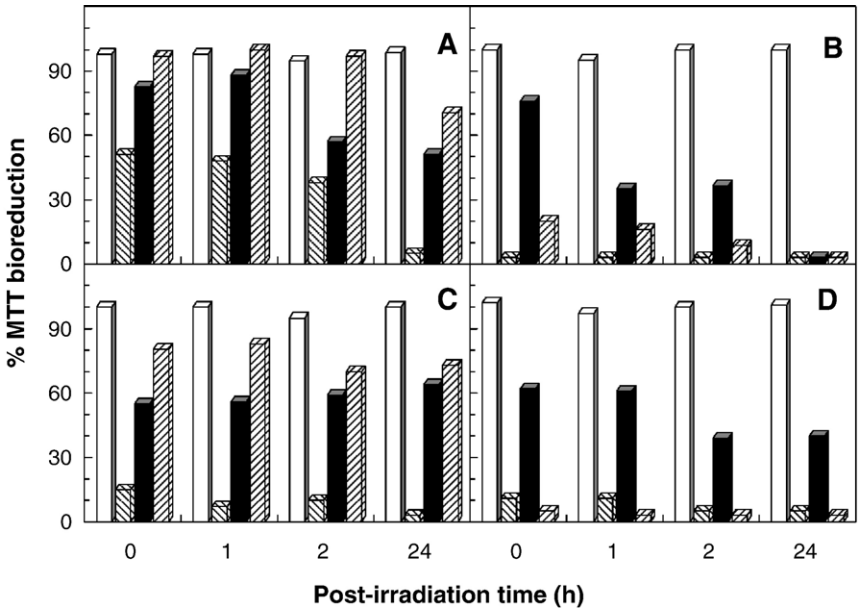

Fig. 8. Photosensitization efficiencies of chlorin derivatives in POPC/OOPS liposomes (A, B) and in DMSO (C, D) measured by the MTT assay. CHL-1 (▧), CHL-2 (▬) and CHL-3 (▨) were added to the wells at 1 μM. The molar ratio of lipid/chlorin derivative was 15:1 for CHL-1 and CHL-2, and 30:1 for CHL-3. After incubation for 1 h (A, C) or 24 h (B, D) in the dark with the chlorins, cell monolayers were irradiated at 660 nm with a fluence of 7.2 J/cm^2. After irradiation, cells were maintained in the dark for 0, 1, 2, and 24 h before each assessment. Samples containing chlorin-free POPC/OOPS liposomes (A, B) or neat DMSO (C, D) were used as negative controls (□). Photosensitization experiments were performed in triplicate and the CV values ranged from 8 to 20%.

in THF solutions. This implies that the high concentration of the chlorins in the liposome bilayer does not negatively affect their photosensitizing ability, nor predetermine their behavior in the cells. As such, the choice of liposomes as carriers would have the additional benefit of a lower phototoxicity of the circulating photosensitizer, given the lower singlet oxygen yields when incorporated in the liposome bilayers with high chlorin-to-lipid molar ratio. This is a desirable feature of a pharmaceutical formulation in order to reduce the risk of side effects.

Using an ultrasensitive singlet oxygen detector, we have been able to record the dynamics of singlet oxygen phosphorescence at 1270 nm photosensitized by the chlorins in the fibroblasts. Given the high reactivity of singlet oxygen towards biomolecules, it can be expected that the chlorins will be able to photosensitize damage to these cells. As a side result, it is interesting to note that singlet oxygen, formed in the cell membrane, is indeed able to escape into the external aqueous phase. This probably means that the chlorins are located very near to the water–lipid interface, not surprising given their polar side chains.

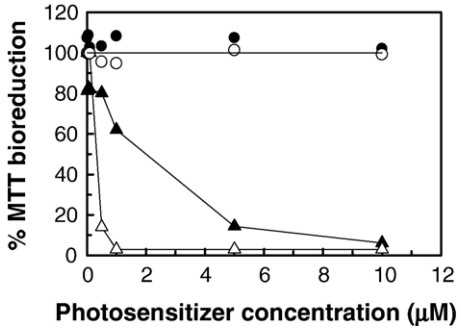

Fig. 9. Comparative photodamage of fibroblasts and HeLa cells after CHL-1-mediated photodynamic treatment. Cells were incubated in the dark for 1 h with different amounts of POPC/OOPS liposomal suspensions either loaded with CHL-1 (△,▲) or empty (○,●). Fibroblasts (○,△) and HeLa cell monolayers (●,▲) were irradiated at 660 nm with a fluence of 7.2 J/cm^2. MTT bioreduction percentage was measured 24 h after irradiation. Photosensitization experiments were performed in triplicate and the CV values ranged from 8 to 20%.

Irrespective of the delivery vehicle used, all the chlorins were non-toxic in the dark but produced extensive cell damage under photodynamic conditions. The efficiency of cell photosensitization depended on the nature of the chlorin and on the cell line, the delivery vehicle, and the length of the pre-incubation period and post-irradiation time. CHL-1 proved the most effective compound, irrespective of the treatment conditions. The photodynamic behavior observed for the three chlorins reflects their relative cellular uptake, which in turn is determined by the nature of their peripheral side chains. Thus, the moderately polar, non-ionic compound CHL-1 shows the highest uptake (Fig. 6) and the highest photodynamic activity (Fig. 8). The negative charge on CHL-2 and the higher hydrophobicity of CHL-3 could account for their lower incorporation into the cells and lower photodynamic efficiency. The effect of the delivery vehicle is best revealed by comparing the efficiency of cell killing by the chlorins incubated for different periods of time. Thus, when the sensitizers were pre-incubated for 1 h, DMSO-delivered chlorins were more effective than liposome-delivered ones. These results agree with the faster uptake of chlorins delivered in DMSO and with observations with other sensitizers

[66,67]. The differences between DMSO and liposomes vanished when the chlorins were pre-incubated for 24 h, and the overall efficiency of cell killing increased. It would seem that the higher uptake of DMSO-delivered chlorins does not translate into higher photodynamic efficiency, probably as a result of a different subcellular localization pattern.

Finally, the photodynamic activity of CHL-1 against two different cell lines was compared. In addition to the efficiency against human skin fibroblasts, CHL-1 was also highly efficient against the cervical adenocarcinoma HeLa cells, although the LD_{50} in HeLa cells (2 μM) was ca. 5-fold higher than in human skin fibroblasts (0.4 μM). These results are in line with those of other sensitizers [47] and reflect the high resistance of HeLa cancer cells [45]. On the other hand, Namiki et al. [69], working with the lipophilic chlorin Ce6 trimethyl ester incorporated in PEG-stealth liposomes and nine kinds of gastric cancer cell lines, obtained values of LD_{80} ranging from 1.9 to 27 μM, which are in line with the LD_{80} values of 0.45 or 4.45 μM obtained by us working with the chlorin CHL-1 and fibroblasts or HeLa cancer cells under similar conditions. Besides, they reported that the LD_{80} values of the Ce6 trimethyl ester incorporated in PEG-stealth liposomes were approximately 50 times smaller than those corresponding to the Ce6 sodium salt, without liposomes. Moreover, the nature of the liposomal carrier is also important since Ichikawa et al. showed that PGEylation enhances the passive targeting of liposomal BDP-MA (benzoporphyrin derivative monoacid) in tumor, but decreases the susceptibility of the drug in PDT [70]. This fact has been taken into account in the design of our liposomal formulations.

In summary, we have established a protocol to incorporate almost quantitatively chlorin photosensitizers into liposomes at concentrations 10-fold larger than in typical formulations. While liposome encapsulation induces important changes in the photophysical properties of photosensitizers, a likely consequence of the high local concentration of the chlorins in the bilayers, it does not impair their cellular uptake or their cell photosensitization ability. In fact, we have observed in the cells the same photophysical behavior as in THF solution. Specifically, we have demonstrated, by recording the near-IR phosphorescence of $^1O_2$, that the chlorins are able to photosensitize the production of $^1O_2$ in the cell membrane. The high photodynamic activity of chlorin-loaded liposomes on a fibroblasts cell model, together with the ability to prepare liposome suspensions containing high chlorin concentrations and the possibility to design liposomal carriers to achieve a specific target site, favors the use of this approach for the extension of these studies to in vivo tumor models as a means to assess the therapeutic efficacy of our formulations.

Acknowledgments

This work was supported by a grant from the EUROPEAN COMMISSION inside the INCO-COPERNICUS 97/98 program (ERBIC15-CT98-0326), by a grant of the Spanish MEC (SAF2002-04034-C02-02), and by a predoctoral fellowship from the University of Barcelona.

References

[1] H. Von Tappeiner, A. Jodlbauer, Die Sensibilisierende Wirkung Fluorieszierender Substanzer. Gesammte Untersuchungen uber die Photodynamische Erscheinung, F. C. W. Vogel, Leipzig, 1907.
[2] M.D. Daniell, J.S. Hill, A history of photodynamic therapy, Aust. N. Z. J. Surg. 61 (1991) 340–348.
[3] R. Ackroyd, C. Kelty, N. Brown, M. Reed, The history of photodetection and photodynamic therapy, Photochem. Photobiol. 74 (2001) 656–669.
[4] C. Hopper, Photodynamic therapy: a clinical reality in the treatment of cancer, Lancet Oncol. 1 (2000) 212–219.
[5] D.E.J.G.J. Dolmans, D. Fukumura, R.K. Jain, Photodynamic therapy for cancer, Nat. Rev., Cancer 3 (2003) 380–387.
[6] T.J. Dougherty, C.J. Gomer, B.W. Henderson, G. Jori, D. Kessel, M. Korbelik, J. Moan, Q. Peng, Photodynamic therapy, J. Natl. Cancer Inst. 90 (1998) 889–905.
[7] O. Ceburkov, H. Golinick, Photodynamic therapy in dermatology, Eur. J. Dermatol. 10 (2000) 568–576.
[8] K. Kalka, H. Merk, H. Mukhtar, Photodynamic therapy in dermatology, J. Am. Acad. Dermatol. 42 (2000) 389–413.
[9] T.J. Dougherty, An update on photodynamic therapy applications, J. Clin. Laser Med. Surg. 20 (2002) 3–7.
[10] T. Kormeili, P.S. Yamauchi, N.J. Lowe, Topical photodynamic therapy in clinical dermatology, Br. J. Dermatol. 150 (2004) 1061–1069.
[11] E. Ben-Hur, N.E. Geacintov, B. Studamire, M.E. Kenney, B. Horowitz, The effect of irradiance on virus sterilization and photodynamic damage in red blood cells sensitized by phtalocyanines, Photochem. Photobiol. 61 (1995) 190–195.
[12] Z. Malik, J. Hanania, Y. Nitzan, New trends in photobiology bactericidal effects of photoactivated porphyrins. An alternative approach to antimicrobial drugs, J. Photochem. Photobiol., B Biol. 5 (1990) 281–293.
[13] K. Brockhorst, T. Els, M. Hoelin-Berlage, Selective enhancement of experimental rat brain tumors with Gd-TPPS, J. Magn. Reson. Imaging 4 (1994) 451–456.
[14] M.R. Niesman, B. Khoobehi, R.L. Magin, A.G. Webb, Liposomes and diagnostic imaging: the potential to visualize both structure and function, J. Lipos. Res. 4 (1994) 741–768.
[15] B.W. Henderson, T.J. Dougherty, How does photodynamic therapy work? Photochem. Photobiol. 55 (1992) 145–157.
[16] R. Bonnett, Photosensitizers of the porphyrin and phthalocyanine series for photodynamic therapy, Chem. Soc. Rev. 24 (1995) 19–33.
[17] M. Niedre, M.S. Patterson, B.C. Wilson, Direct near-infrared luminescence detection of singlet oxygen generated by photodynamic therapy in cells in vitro and tissues in vivo, Photochem. Photobiol. 75 (2002) 382–391.
[18] R. Bonnett, Chemical Aspects of Photodynamic Therapy, Gordon and Breach Science Publishers, Amsterdam, 2000, pp. 115–128.
[19] D. Brault, B. Aveline, O. Delgado, M.T. Martin, Chlorin-type photosensitizers photochemically derived from vinyl porphyrins, Photochem. Photobiol. 73 (2001) 331–338.
[20] K. Das, B. Jain, A. Dube, P.K. Gupta, pH dependent binding of chlorin-p6 with phosphatidylcholine liposomes, Chem. Phys. Lett. 401 (2005) 185–188.
[21] F. Rancan, A. Wiehe, M. Nöbel, M.O. Senge, S. Al Omari, F. Böhm, M. John, B. Röder, Influence of substitutions on asymmetric dihydroxychlorins with regard to intracellular uptake, subcellular localization and photosensitization of Jurkat cells, J. Photochem. Photobiol., B Biol. 78 (2005) 17–28.
[22] E.S. Nyman, P.H. Hynninen, Research advances in the use of tetrapyrrolic photosensitizers for photodynamic therapy, J. Photochem. Photobiol., B Biol. 73 (2004) 1–28.
[23] D. Wohrle, A. Hirth, T. Bogdahn-Rai, G. Schnurofeil, M. Shopova, Photodynamic therapy of cancer: second and third generation of photosensitizers, Russ. Chem. Bull. 47 (1998) 807–816.
[24] A.S.L. Derycke, P.A.M. De Witte, Transferrin-mediated targeting of hypericin embedded in sterically stabilized PEG-liposomes, Int. J. Oncol. 20 (2002) 181–187.
[25] G. Zhang, A. Harada, N. Nishiyama, D. Jiang, H. Koyama, T. Aida, K. Kataoka, Polyion complex micelles entrapping cationic dendrimer

porphyrin: effective photosensitizer for photodynamic therapy of cancer, J. Control. Release 93 (2003) 141–150.
[26] E. Reddi, Role of delivery vehicles for photosensitizers in the photodynamic therapy of tumors, J. Photochem. Photobiol., B Biol. 37 (1997) 189–195.
[27] Y.N. Konan, R. Gurny, E. Allémann, State of the art in the delivery of photosensitizers for photodynamic therapy, J. Photochem. Photobiol., B Biol. 66 (2002) 89–106.
[28] K. Woodburn, C.K. Chang, S.W. Lee, B. Henderson, D. Kessel, Biodistribution and PDT efficacy of a ketochlorin photosensitizer as a function of the delivery vehicle, Photochem. Photobiol. 60 (1994) 154–159.
[29] U. Isele, K. Schieweck, R. Kessler, P.V. Hoogevest, H. Capraro, Pharmacokinetics and body distribution of liposomal zinc phthalocyanine in tumor-bearing mice: influence of aggregation state, particle size, and composition, J. Pharm. Sci. 84 (1995) 166–173.
[30] J. Kreuter, Colloidal Drug Delivery Systems, Marcel Dekker, Inc., New York, 1994.
[31] T.M. Allen, P.R. Cullis, Drug delivery systems: entering the mainstream, Science 303 (2004) 1818–1822.
[32] M. Hashida, S. Kawakami, F. Yamashita, Lipid carrier systems for targeted drug and gene delivery, Chem. Pharm. Bull. 53 (2005) 871–880.
[33] X. Damoiseau, H.J. Schuitmaker, J.W.M. Lagerberg, M. Hoebeke, Increase of the photosensitizing efficiency of bacteriochlorin *a* by liposome-incorporation, J. Photochem. Photobiol., B Biol. 60 (2001) 50–60.
[34] K. Lang, J. Mosinger, D.M. Wagnerová, Photophysical properties of porphyrinoid sensitizers non-covalently bound to host molecules; models for photodynamic therapy, Coord. Chem. Rev. 248 (2004) 321–350.
[35] A. Lavi, H. Weitman, R.T. Holmes, K.M. Smith, B. Ehrenberg, The depth of porphyrin in membrane and the membrane's physical properties affect the photosensitizing efficiency, Biophys. J. 82 (2002) 2101–2110.
[36] M. Hoebeke, The importance of liposomes as models and tools in the understanding of photosensitization mechanisms, J. Photochem. Photobiol., B Biol. 28 (1995) 189–196.
[37] L. Bourré, S. Thibaut, M. Fimiani, Y. Ferrand, G. Simonneaux, T. Patrice, In vivo photosensitizing efficiency of a diphenylchlorin sensitizer: interest of a DMPC liposome formulation, Pharmacol. Res. 47 (2003) 253–261.
[38] A. Igarashi, H. Konno, T. Tanaka, S. Nakamura, Y. Sadzuka, T. Hirano, Y. Fujise, Liposomal photofrin enhances therapeutic efficacy of photodynamic therapy against the human gastric cancer, Toxicol. Lett. 145 (2003) 133–141.
[39] A.S.L. Derycke, P.A.M. Witte, Liposomes for photodynamic therapy, Adv. Drug Delivery Rev. 56 (2004) 17–30.
[40] D.D. Lasic, D. Papahadjopoulos, Medical Applications of Liposomes, Elsevier Science BV, Amsterdam, 1998.
[41] F. Postigo, M. Mora, M.A. de Madariaga, S. Nonell, M.L. Sagristá, Incorporation of hydrophobic porphyrins into liposomes: characterization and structural requirements, Int. J. Pharm. 278 (2004) 239–254.
[42] F. Ricchelli, Photophysical properties of porphyrins in biological membranes, J. Photochem. Photobiol., B Biol. 29 (1995) 109–118.
[43] M.L. Agarwal, M.E. Clay, E.J. Harvey, H.H. Evans, A.R. Antunez, N.L. Oleinick, Photodynamic therapy induces rapid cell death by apoptosis in L5178Y mouse lymphoma cells, Cancer Res. 51 (1991) 5993–5996.
[44] Y. Luo, C.K. Chang, D. Kessel, Rapid initiation of apoptosis by photodynamic therapy, Photochem. Photobiol. 63 (1996) 528–534.
[45] J. Zhang, E.H. Cao, J.F. Li, T.C. Zhang, W.J. Ma, Photodynamic effects of hypocrellin A on three human malignant cell lines by inducing apoptotic cell death, J. Photochem. Photobiol., B Biol. 43 (1998) 106–111.
[46] W.S. Ahn, S.M. Bae, S.W. Huh, J.M. Lee, S.E. Namkoong, S.J. Han, C.K. Kim, Necrosis-like death with plasma membrane damage against cervical cancer cells by photodynamic therapy, Int. J. Gynecol. Cancer 14 (2004) 475–482.
[47] Z. Tong, G. Singh, A.J. Raibow, The role of p53 tumor suppressor in the response of human cells to photofrin-mediated photodynamic therapy, Photochem. Photobiol. 71 (2000) 201–210.
[48] S.-H. Wu, Q.-G. Ren, M.-O. Zhou, Y. Wei, J.-Y. Chen, Photodynamic effects of 5-aminolevulinic acid and its hexylester on several cell lines, Acta Biochim. Biophys. Sin. 35 (2003) 660–665.
[49] R. Abraham, A.E. Rowan, N.W. Smith, K.M. Smith, NMR spectra of the porphyrins. Part 42. [1]The synthesis and aggregation behaviour of some chlorophyll analogues, J. Chem. Soc., Perkin Trans. 2 (1993) 1047–1059.
[50] K.M. Smith, D.A. Goff, D.J. Simpson, *Meso* substitution of chlorophyll derivatives: direct route for transformation of bacteriopheophorbides *d* into bacteriopheophorbides *c*, J. Am. Chem. Soc. 107 (1985) 4946–4954.
[51] F. Postigo, Delivery of photosensitizers by means of liposomes. Application to photodynamic sterilization of blood and to photodynamic therapy of cancer. PhD thesis (2005) University of Barcelona, Spain.
[52] S.L. Murov, I. Carmichael, G.L. Hug, Handbook of Photochemistry, Marcel Dekker, New York, 1993, pp. 1–420.
[53] S. Nonell, S.E. Braslavsky, Time-resolved singlet oxygen detection, in: L. Packer, H. Sies (Eds.), Methods in Enzymology, vol. 319, Singlet Oxygen, UV-A and Ozone, Academic Press, USA, 2000, pp. 37–49.
[54] F.W. Wilkinson, W.P. Helman, A.B. Ross, Quantum yields for the photosensitized formation of the lowest electronically excited singlet state of molecular oxygen in solution, J. Phys. Chem. 22 (1993) 113–262.
[55] J.B. Verlhac, A. Gaudemer, Water-soluble porphyrins and metalloporphyrins as photosensitizers in aerated aqueous solutions: I. Detection and determination of quantum yield of formation of singlet oxygen, Nouv. J. Chim. 8 (1984) 401–406.
[56] Y. Usui, K. Kamaogawa, A standard system to determine the quantum yield of singlet oxygen formation in aqueous solution, Photochem. Photobiol. 19 (1974) 245–247.
[57] P. Ziolkowski, M. Jelén, P. Marszalik, E. Piasecki, M.A. Vallés, D.B. Berezin, A. El Merouani, A.M. Gómez, V. Pérez, R. Bonnett, P.A. Shatunov, R.M. Pintó, S. Caballero, M.A. De Madariaga, M. Mora, M.L. Sagristá, F. Postigo, O.I. Koifman, A.S. Semeykin, PDT photosensitizers for blood sterilization: viruses photoinactivation and red blood cells toxicity assays, in: O.A. Golubchikov (Ed.), Porphyrin Chemistry Advances, vol. 3, The Scientific Research Institut of Chemistry, Saint Petersburg, 2001, pp. 179–190.
[58] T. Mosmann, Rapid colorimetric assay for cellular growth and survival: application to proliferation and cytotoxicity assays, J. Immunol. Methods 65 (1983) 55–63.
[59] C. Grewer, G. Schermann, R. Schmidt, A. Volcker, H.D. Brauer, A. Meier, F.P. Montforts, Potential photosensitizers for photodynamic therapy III. Photophysical properties of a lipophilic chlorin and its zinc and tin chelates, J. Photochem. Photobiol., B Biol. 11 (1991) 285–293.
[60] R.K. Pandey, A.B. Sumlin, S. Constantine, M. Aoudia, W.R. Potter, D.A. Bellnier, B.W. Henderson, M.A. Rodgers, K.M. Smith, T.J. Dougherty, Alkyl ether analogs of chlorophyll-a derivatives: 1. Synthesis, photophysical properties and photodynamic efficacy, Photochem. Photobiol. 64 (1996) 194–204.
[61] R.W. Redmond, J.N. Gamlin, A compilation of singlet oxygen yields from biologically relevant molecules, Photochem. Photobiol. 70 (1999) 391–475.
[62] X. Damoiseau, F. Tfibel, M. Hoebeke, M.P. Fontaine-Aupart, Effect of aggregation on bacteriochlorin a triplet-state formation: a laser flash photolysis study, Photochem. Photobiol. 76 (2002) 480–485.
[63] G. Valduga, S. Nonell, E. Reddi, G. Jori, S.E. Braslavsky, The production of singlet molecular oxygen by zinc (II) phthalocyanine in ethanol and in unilamellar vesicles. Chemical quenching and phosphorescence studies, Photochem. Photobiol. 48 (1988) 1–5.
[64] R.W. Redmond, G. Valduga, S. Nonell, S.E. Braslavsky, K. Schaffner, E. Vogel, K. Pramod, M. Köcher, The photophysical properties of porphycene incorporated in small unilamellar lipid vesicles, J. Photochem. Photobiol., B Biol. 3 (1989) 193–207.
[65] S. Nonell, S.E. Braslavsky, K. Schaffner, Quantum yield of production of singlet molecular oxygen ($^1\Delta_g$) in aqueous dispersions of small unilamellar lipid vesicles. A time-resolved near-IR phosphorescence study, Photochem. Photobiol. 51 (1990) 551–556.
[66] Z.J. Wang, Y.Y. He, C.G. Huang, J.S. Huang, Y.C. Huang, J.Y. An, Y. Gu, L.J. Jiang, Pharmacokinetics, tissue distribution and photodynamic therapy efficacy of liposomal-delivered hypocrellin A, a potential photosensitizer for tumor therapy, Photochem. Photobiol. 70 (1999) 733–780.

[67] F. Rancan, A. Wiehe, M. Nöbel, M.O. Senge, A. Al Omari, F. Böhm, M. John, B. Röder, Influence of substitutions on asymmetric dihydroxychlorins with regard to intracellular uptake, subcellular localization and photosensitization of Jurkat cells, J. Photochem, Photobiol., B 78 (2005) 17–28.
[68] NOVARTIS Pharmaceutical USA, http://www.pharma.us.novartis.com/product/pi/pdf/visudyne.pdf, 2005.
[69] Y. Namiki, T. Namiki, M. Date, K. Yanagihara, M. Yashiro, H. Takahashi, Enhanced photodynamic antitumor effect on gastric cancer by a novel photosensitive stealth liposome, Pharmacol. Res. 50 (2004) 65–76.
[70] K. Ichikawa, T. Hikita, N. Maeda, Y. Takeuchi, Y. Namba, N. Oku, PEGylation of liposome decreases the susceptibility of liposomal drug in cancer photodynamic therapy, Biol. Pharm. Bull. 27 (2004) 443–444.